International Journal of Current Science Research and Review
ISSN: 2581-8341
Volume 07 Issue 07 July 2024
DOI: 10.47191/ijcsrr/V7-i7-54, Impact Factor: 7.943
IJCSRR @ 2024
www.ijcsrr.org

Michelson, Morley and Sagnac Experiments Further Elaboration

Bagrat Melkoumian

Engineering Physics Institute of Samarkand State University named after Sharof Rashidov,
15 University Boulevard, Samarkand, UZ

ABSTRACT: Michelson, Morley and Sagnac experiments are interpreted. The main properties of the laser gyroscopes are considered, including the maximum sensitivity, the impact of the non-plane wave fronts and the impact of precession of moment vector of radiation on the laser gyro output. Autonomous resonatory sensor – a new type of linear laser accelerometer - has been created based on a linear laser rather than ring resonators. The proposed device operates without any straining or moving parts and uses standing wave of the coherent radiation in the resonator as the sensor of accelerated movement.

KEY WORDS: laser accelerometer, laser gyro, navigation, linear and ring lasers, physical and quantum optics.

1. KNOWN OPTICAL EFFECTS IN ACCELERATED RESONATORS

We consider influence of external forces on the radiation in rigid resonator with an invariable geometry that has all its elements and a photodetector stationary relative to each other during the interaction time, which leads to an accelerated motion of the resonator with a radiation. We consider the radiation medium to be stationary and uniform in the intrinsic frame of reference of the resonator, when the dielectric ε and the magnetic μ permeability are constant.

Any movement of radiation source and receiver relative to each other, or any movement of the active medium [1] in the cavity due to the influence of external forces, additionally leads to Doppler, or Fresnel-Fizeau effects [2-3].

Prior to our works, there were two known phenomena of "optical dynamics" in moving rigid resonators, independent of a medium: The first one is *the invariability of radiation parameters* of a source in a form of the cross-shaped interferograph, as in Fig. 1, that is moving with orbital velocity of the Earth. It discovered by Albert Abraham Michelson and his colleagues [4-6].

The second one is *the appearance of a frequency shift proportional to the angular velocity of rotation* of the ring resonator for each component of its radiation. It was the most fully investigated in [7-11] by Georges Marc Marie Sagnac. Both phenomena have been examined to test the hypothesis of "ether dragging" [12].

1.1 Cross-Shaped Michelson Interferograph

Michelson and his colleagues have created a new optical setup to measure "ether vortices". A cruciform interferograph was assembled in a wine cellar, on a stone slab (1.5 x 1.5 x 0.3) m^3, floating on a mercury "pillow" [12], as in Fig. 1.

Furthermore, the measuring "shoulder" of the cross-shaped beam contour of the linear interferograph was directed along the motion of the Earth, and then perpendicular to it. However, a shift of the interference fringes on the screen, that was expected per "ether" hypothesis, was not found neither in the first experiment in 1881, nor after.

It should not have been, but for other reasons - reasons not related to presence or absence of the "ether".

The Fig. 1 shows a diagram of an interferograph for measuring the assumed "ether vortices" during the translational movement of the installation together with the Earth in its orbit. Its elements remained motionless relative to each other throughout the measurement.

The interference picture on the screen of the new setup appeared to be very sensitive to any shifts between its elements. The "wrong" interferograph with a moving element, or with a moving optically dense medium, became an "interferometer" - a precision instrument for many applications. Until recently, Michelson interferometers were widely used in rotation stabilization systems of optical disk drives (CD-ROM) in millions of copies.

International Journal of Current Science Research and Review
ISSN: 2581-8341
Volume 07 Issue 07 July 2024
DOI: 10.47191/ijcsrr/V7-i7-54, Impact Factor: 7.943
IJCSRR @ 2024
www.ijcsrr.org

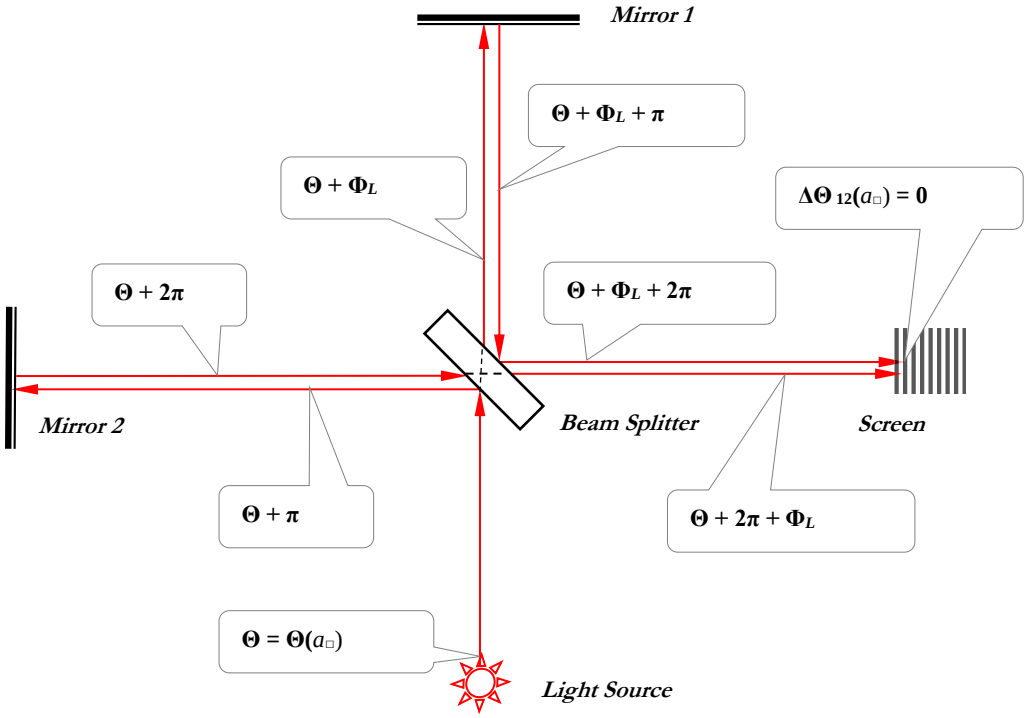

Fig. 1. Optical scheme of Michelson's "interferograph" (1881-1886).

1.2 Interpretation of the Michelson's First Experiments

Before our work, the negative result of Michelson's first experiments, or the invariability of radiation parameters in a cruciform interferograph, was explained by the fact that the ether, as a special physical medium, does not exist. On the other hand, a stable effect was found in a Sagnac ring interferograph on a similar plate - the appearance of a frequency shift proportional to the angular velocity of rotation of the ring resonator.

Nevertheless, the absence of an observable change in the interference pattern on the output of the setup according to Fig. 1 allows for a different explanation based on a general physics [13-16].

The absence of interference fringes shifting on the screen of a linear (cross-shaped) interferograph does not contradict the laws of classical physics and in no way relates to a presence or absence of the "ether".

Let us review what done in these experiments. On a freely floating slab, the researchers had a fixed light source, a fixed light receiver, and fixed framing elements (mirrors and beam splitter), all within a closed system that was left to itself and moved in a uniform rectilinear motion during their measurements. The orbital motion of the Earth around the Sun is the best available example of a uniform rectilinear motion for small terrestrial objects in a short experiment time. According to Galileo Galilei (1564-1642), a physical system is capable to detect only a change of its speed (change of its state) during an uneven motion (caused by an external influence).

In addition, one can show that at the output of the cross-shaped interferograph, a "zero path difference" is observed between two components of the same beam (Fig. 1). This design compensates for any change in the phase of a beam due to uneven movement of the entire system. In the first Michelson interferograph, the initial beam from the source is split into two (opposite in phase), each of which undergoes same number of reflections, on its way to the screen. In addition, it cannot be expected, that electromagnetic radiation without mass (in *kg*), but with its *eigenvalues* of energy, momentum, or angular momentum, changes its space-time characteristics in the same way as a material point does.

Michelson did not measure the orbital velocity of the Earth's motion in the first relevant works for four reasons:

International Journal of Current Science Research and Review
ISSN: 2581-8341
Volume 07 Issue 07 July 2024
DOI: 10.47191/ijcsrr/V7-i7-54, Impact Factor: 7.943
IJCSRR @ 2024
www.ijcsrr.org

1) The absence of a shift of the fringes of the interference pattern on the *Screen* of Michelson's "interferograph" does not contradict the general physics. The system was closed, left to itself, and moved with the Earth in almost a uniform rectilinear motion during the entire experiment in the orbit around the Sun.
2) According to Maxwell's theory, the radiation from the *Light Source* is divided by the *Beam Splitter* plate into 2 sleeves from the *Beam Splitter* to *Mirror 1* and to *Mirror 2*. The beams pass back and forth and meet on the *Screen* after an equal number of reflections, with equal phases and with zero phase difference.
3) The light in the resonator should not be sensitive to the movement of the common plate *along the standing radiation wave*. This would have been the case only if the source produces of outgoing massive balls. For example, an axis of acceleration sensitivity of the "autonomous resonatory sensor" (ARS) is directed almost at a right angle to the standing light wave in the resonator, which is determined by the direction of the "vector of radiation" [13-14].
4) According to our theory for ARS [15-16], the Michelson's interferograph circuit compensates for any possible change in the phase of the radiation that is including a case of uneven motion of the entire system [15-16].
Previously, we used the term autonomous resonatory device (ARD). Next, we will call the new laser accelerometer, as in the patent [21]: autonomous resonatory sensor (ARS).
It can be assumed that with the movement of the entire installation plate, a phase of the radiation from the *Light Source* would change, determined by the acceleration of the plate, i.e., by $\Theta(\boldsymbol{a}_{\square})$, where $\boldsymbol{a}_{\square}$ - is the acceleration of the installation plate (□). Further, the phase of light in the arms of the interferometer changes by (π) after each reflection and by phase (Φ_L) after each pass of the "*Beam Splitter*", where *L* is the length of the optical path traveled in the plate. As a result, we get zero phase difference at the output.

1.3 Ring Resonator Based Devices

Michelson, A.A., Harress, F. and Sagnac, G.M.M. made the first attempts of autonomous motion measurements by an optical apparatus without straining or moving parts [12]. Michelson did not measure the linear velocity of motion along the Earth's orbit with a cruciform interferograph on a mercury pillow (1881-1887), however, by making one of its elements movable, invented the first interferometer.
Harress measured the Fresnel entrainment of light in rotating disks of glass (1911) and discovered a beat signal that he did not expect, later become known as the Sagnac effect, who studied it thoroughly (1912-1914).
For a purposeful measurement of a rotational motion, Sagnac invented a "ring interferograph", as in Fig. 2. Here mirrors A, B, C, a translucent plate D, a light source Q and a photodetector P are all fixed on a table, which is rotated on a mercury "pillow" with an angular velocity Ω. The light beam from Q is split by the plate D into two beams - DABCDP and DCBADP. These light beams, running around the ABCD contour in opposite directions, form a ring standing wave and interfere at P.

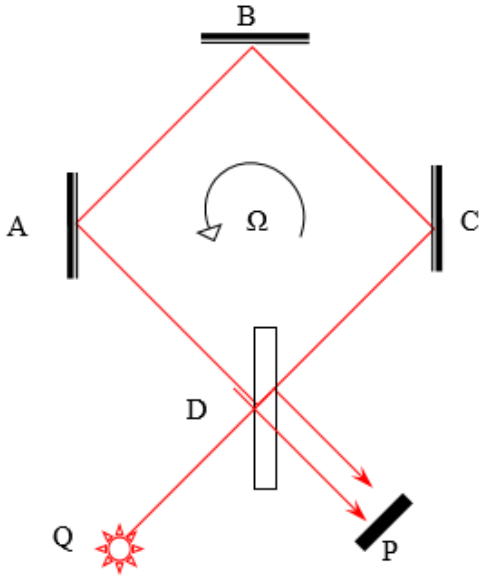

Fig. 2. Optical scheme of the Sagnac experiment (1913-1914).

International Journal of Current Science Research and Review
ISSN: 2581-8341
Volume 07 Issue 07 July 2024
DOI: 10.47191/ijcsrr/V7-i7-54, Impact Factor: 7.943
IJCSRR @ 2024
www.ijcsrr.org

Sagnac, having shown that "the ether is not carried away by a rotating system", measured the angular velocity of rotation of the table $\Omega \geq 30$ °/s and proposed a formula (1), that had a good (1/100) agreement with the experimental data for large Ω.

$$\Delta\nu = \frac{4 \cdot S \cdot \Omega}{\lambda \cdot L} \qquad (1)$$

Here in (1) L is the length of the perimeter of an axial contour of the resonator; S is the area bounded by the contour of the resonator; Ω is the measured angular velocity; λ is the wavelength of radiation in the resonator before its rotation. It can be shown that (1) is performed only for plane waves with an infinite phase front.

At lower speeds Sagnac found a "dead zone", or "capture zone" and could not measure the small angular velocity of the Earth's daily rotation, which is not prohibited by (1).

Any physical system with its own momentum of pulse in a frame of reference rotating with Ω, has the intrinsic energy (2), which is determined through its energy $\hat{\varepsilon}_0$ in the inertial system, in the general case, as an operator relation

$$\hat{\varepsilon} = \hat{\varepsilon}_0 - \left(\widehat{\mathbf{M}} \cdot \boldsymbol{\Omega}\right). \qquad (2)$$

The "capture zone" of laser gyro (LG) necessitates additional alternating bias devices (mechanical or electromagnetic) to be attached to an active or passive ring resonator.

The relation (3) of light energy changes for co- and contra rotation propagating light waves in ring resonator will be

$$(\Delta\varepsilon)_{2;1} = \varepsilon_{2;1} - \varepsilon_0 = \pm\left(\widehat{\mathbf{M}} \cdot \boldsymbol{\Omega}\right). \qquad (3)$$

2. EXPLANATION OF OPTICAL EFFECTS OF THE RING STANDING LIGHT WAVE BASED ON PRINCIPLES OF CLASSICAL QUANTUM MECHANICS AND ELECTRODYNAMICS

It was found [17] that the "dead zone", or "capture zone" of LG (see Fig. 3) is determined by the measurement conditions of Ω, and with low-quality LG elements and insufficient electro-vacuum treatment of the resonator, when one cannot achieves a stable generation, or may even lose generation, without the external impact of rotation.

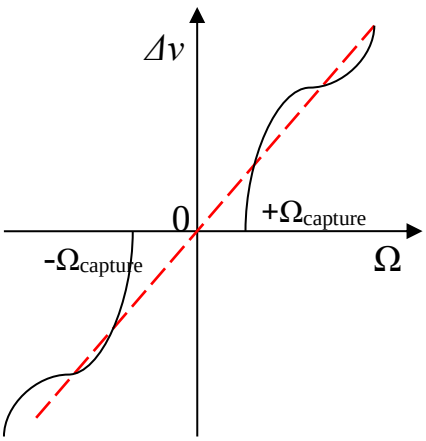

Fig. 3. Output characteristics of LG.

In Fig. 3 the values $\pm\Omega_{capture}$ are the minimum values of Ω, measured using the LG monoblock installed on the stand, when it rotates in different directions around an axis perpendicular to the plane of the radial contour. The variable range between them is the "capture zone" of LG. Output characteristic of LG according to (1) is represented by a red dotted line, and the usual experimental characteristic are represented by black solid lines.

International Journal of Current Science Research and Review
ISSN: 2581-8341
Volume 07 Issue 07 July 2024
DOI: 10.47191/ijcsrr/V7-i7-54, Impact Factor: 7.943
IJCSRR @ 2024
www.ijcsrr.org

Already classical interpretation in our work makes it possible to determine the meaning of (1) and to develop recommendations for developers of the precision technology.

Heer, C.V. [18] and Skrotsky. G.V. [19] also have suggested that equation (2) can be applied to a quasi-classical analysis of the Sagnac effect in a ring resonator, however corresponding analysis was not presented.

We have defined the classical *angular momentum of pulse* (4) for a photon with a wave vector **k**, as

$$\boldsymbol{\mu} = \hbar \cdot [\boldsymbol{r} \times \boldsymbol{k}] \qquad (4)$$

This vector of angular momentum of pulse is indeterminate for a free photon or for a plane electromagnetic wave. However, for a standing wave with a wavelength λ and with almost a flat front in a ring resonator of LG, the quantum-determined value for one of its components will be **M** - the angular momentum of pulse averaged over the circumvention time T of a resonator with a perimeter L, in the form of

$$\mathbf{M} = \int_0^T \boldsymbol{\mu} \cdot \frac{dt}{T} = \frac{\hbar}{L} \oint [\boldsymbol{r} \times \boldsymbol{k}] \cdot dl = \frac{2\pi \cdot \hbar}{\lambda \cdot L} \cdot \int_0^L [\boldsymbol{r} \times d\boldsymbol{l}] \qquad (5)$$

Considering the relation of light energy changes $(\Delta E = E - E_0)$ with a change in its frequency $(\Delta E = 2\pi\hbar \cdot \Delta\nu)$, we obtain frequency shifts for components 2 and 1 of the standing wave with momentum of pulse $\mathbf{M}_2 = -\mathbf{M}$, against $\boldsymbol{\Omega}$, and $\mathbf{M}_1 = \mathbf{M}$, along $\boldsymbol{\Omega}$, accordingly

$$(\Delta\nu)_{2,1} = \pm \frac{(\mathbf{M} \cdot \boldsymbol{\Omega})}{2\pi \cdot \hbar} = \pm \frac{2 \cdot (\mathbf{S} \cdot \boldsymbol{\Omega})}{\lambda \cdot L} \qquad (6)$$

The Sagnac formula determines the difference in frequency shifts ($\Delta\nu_2 - \Delta\nu_1$) by (6) as

$$\Delta\nu = 2 \cdot \frac{(\mathbf{M} \cdot \boldsymbol{\Omega})}{2\pi \cdot \hbar} = \frac{4 \cdot (\mathbf{S} \cdot \boldsymbol{\Omega})}{\lambda \cdot L} \qquad (7)$$

Formula (7) for the Sagnac effect is due to the presence of certain moments of pulse for each component of a ring standing wave in the LG.

According to the relation (5) between $\boldsymbol{k}$ and $\mathbf{M}$, the permissible precession of the vector $\mathbf{M}$ in its own frame of reference (if it is the present moment of the pulse) around a certain direction of angular velocity is equivalent to a change in the polarization state of the components of the ring standing wave.

The area vector $\mathbf{S}$ defines the "technological" axis of LG sensitivity. This is useful, since with the precession of $\mathbf{M}$ around $\mathbf{S}$, we would separate a fixed axis of the reference system of the laser gyroscope and a variable multiplier.

2.1 Quantum Limit of the Sagnac Effect

In our earlier works, the maximum sensitivity of the LG was obtained, limited by the uncertainty relations of quantum mechanics "energy – time" or "number of photons – phase", that connects experimentally observed parameters of the LG. From (7) the angular momentum of pulse of one component of the ring wave is

$$\mathbf{M} = h \frac{2}{\lambda L} \mathbf{S} = h \frac{R_{eff}}{\lambda} \hat{\mathbf{s}}, \qquad (8)$$

where the direction of the area vector $\mathbf{S}$ is determined by the wave vector $\boldsymbol{k}$ according to the right-hand screw rule, $\hat{\mathbf{s}}$ is ort in direction $\mathbf{S}$, and $(R_{eff} = 2S/L)$ is the radius of a circle inscribed in the axial contour of the ring resonator.

From (2) and (8), the energy change for each (1 or 2) of oppositely propagating ring waves due to the rotation of the ring laser resonator is equal to

$$(\Delta\varepsilon)_{1;2} = \varepsilon_0 - \varepsilon_{1;2} = \pm h \frac{2}{\lambda L} (\mathbf{S} \cdot \boldsymbol{\Omega}) \qquad (9)$$

Considering (9) and the uncertainty relation for the change in the energy of component 1 of the standing wave during its rotation, at the measurement time $\delta t = T$, we obtain the uncertainty of the energy measurement

International Journal of Current Science Research and Review
ISSN: 2581-8341
Volume 07 Issue 07 July 2024
DOI: 10.47191/ijcsrr/V7-i7-54, Impact Factor: 7.943
IJCSRR @ 2024
www.ijcsrr.org

$$\delta(\Delta\varepsilon_1) = \delta\left(h\frac{2}{\lambda L}(\mathbf{S}\cdot\mathbf{\Omega})\right) \geq \frac{\hbar}{T} \qquad (10)$$

Since $(\mathbf{S}\cdot\mathbf{\Omega}) = S\Omega\ (\hat{\mathbf{s}}\cdot\hat{\boldsymbol{\omega}})$, we have for the angular velocity module the condition

$$\delta(\Omega) \geq \frac{\lambda}{2\pi R_{eff}\cdot T}(\hat{\mathbf{s}}\cdot\hat{\boldsymbol{\omega}})^{-1} \qquad (11)$$

where $\hat{\boldsymbol{\omega}}$ is ort in direction of vector $\mathbf{\Omega}$.
It is obvious that the obtained relation (11) for the theoretical limit of the minimum uncertainty in angular velocity measurements also determines the minimum recorded angular velocity $(\Omega_{\min})$, since $\Omega_{\min} \geq \delta(\Omega)$.
Otherwise, the measured value is less than the maximum achievable accuracy, which makes no sense. Corresponding to relation (11) the minimum uncertainty of the angle of rotation will be

$$\delta(\varphi) \geq \frac{\lambda}{2\pi R_{eff}}(\hat{\boldsymbol{s}}\cdot\hat{\boldsymbol{\omega}})^{-1} \qquad (12)$$

For two components (12) will be halved. The uncertainty of the angle $\delta(\varphi)_2$ in the scheme with two wave components is equal to the ratio of half the wavelength of radiation in a stationary ring resonator $(c/2)$ to the circumference $(2\pi\cdot R_{eff})$ inscribed in its axial contour:

$$\delta(\varphi)_2 \geq \frac{\lambda}{4\pi R_{eff}}(\hat{\boldsymbol{s}}\cdot\hat{\boldsymbol{\omega}})^{-1} \qquad (13)$$

The maximum sensitivity of LG calculated by (13) proved to be practically achievable and somewhat lower than previously assumed.
It should be noted that the "energy-time" relation is introduced for reasons of energy fluctuations and is not, in a strict sense, an uncertainty relation of quantum mechanics, since time (t) is not an operator, but a parameter. We obtain (11) and (12) also from the uncertainty relation for the "photon number" and "phase" operators. The phase operator $(\hat{\varphi})$ introduced by Dirac, by analogy with the classical phase, together with the annihilation operator

$$\hat{a} = (\hat{n})^{1/2}\cdot\exp(i\hat{\varphi}), \qquad (14)$$

where $(\hat{n})$ is the particle number operator. The uncertainty "photon number – phase" has the form

$$\delta(n)\cdot\delta(\varphi) \geq \frac{1}{2}. \qquad (15)$$

Considering a minimum change in the number of photons and a minimum change of the phase of light when the ring laser rotates, the change in the radiation phase $d\Phi$ on the element dL of the resonator contour during the resonator rotation is determined from the expression

$$d\Phi = k\,dL + (\boldsymbol{k}\cdot[\mathbf{\Omega}\times\mathbf{r}])\,\frac{dL}{c} \qquad (16)$$

In (16), as in (5), the vector $\boldsymbol{k}$ directed along the element dL of the resonator contour, so there are no arrows in the first term of the right side (16). Here $\mathbf{r}$ is the radius vector of the element dL relative to the origin. For a complete circumvention of the ring resonator, the phase of one component of the standing wave will change as

$$\Phi = 2\pi N_\lambda + \left((\mathbf{\Omega}/c)\cdot\oint[\mathbf{r}\times\boldsymbol{k}]\,dL\right) \qquad (17)$$

International Journal of Current Science Research and Review
ISSN: 2581-8341
Volume 07 Issue 07 July 2024
DOI: 10.47191/ijcsrr/V7-i7-54, Impact Factor: 7.943
IJCSRR @ 2024
www.ijcsrr.org

where $N_\lambda = L/\lambda$ is the number of wavelengths placed along the perimeter of the ring laser resonator, and a cyclic permutation is made in the mixed vector product of (16). Using (5) and (8), we transform (17) into

$$\Phi = 2\pi N_\lambda \left(1 + \frac{(\mathbf{M}\cdot\boldsymbol{\Omega})}{h\nu}\right) \qquad (18)$$

From (18), considering (8), the phase change of one of the components of the standing radiation wave in the resonator of the ring laser due to rotation is equal to

$$\Delta(\Phi)_\Omega = 2\pi N_\lambda \frac{(\mathbf{M}\cdot\boldsymbol{\Omega})}{h\nu} = \frac{2\pi R_{eff}}{\lambda}\,\Omega\,(\hat{\boldsymbol{\mu}}\cdot\hat{\boldsymbol{\omega}})\,\frac{L}{c} \qquad (19)$$

where $\hat{\boldsymbol{\mu}}$ is the ort in the direction of the momentum vector $\mathbf{M}$. The energy of the wave packet state defined as

$$\varepsilon_n = h\nu\left(n + \frac{1}{2}\right). \qquad (20)$$

Therefore, the minimum value of the change in the number of photons is considered equal to

$$\delta(n)_{\min} = \frac{1}{2} \qquad (21)$$

In this case, substituting the changes (21) and (19) in (15), we get

$$\delta(n)_{\min}\cdot\delta\left(\frac{2\pi R_{eff}}{\lambda}\,\Omega\,(\hat{\boldsymbol{\mu}}\cdot\hat{\boldsymbol{\omega}})\,\frac{L}{c}\right)_{\min} \geq \frac{1}{2} \qquad (22)$$

From (22) the minimum value for the module of angular velocity of rotation estimated as

$$\delta(\Omega)_{\min} \geq \frac{\lambda}{2\pi\cdot R_{eff}}\cdot(\hat{\boldsymbol{\mu}}\cdot\hat{\boldsymbol{\omega}})^{-1}\cdot\frac{c}{L} \qquad (23)$$

The value (23) is determined for one circumvention of the resonator perimeter L of a ring laser by one wave packet. It is equivalent to (11) since it is obvious that $(L = cT)$ and $(\hat{\boldsymbol{\mu}} = \hat{\mathbf{s}})$.

Substituting (R_{eff}) from (8) into the inequality (12) multiplied by h, we see that sensitivity limit of LG is determined by the uncertainty ratio for the projection of the angular momentum (M_Ω) of a ring wave of light and the projection of the rotation angle vector (Φ_Ω) of a ring resonator on the axis of rotation (Ω), as in (24).

$$h\frac{R_{eff}}{\lambda}(\hat{\mathbf{s}}\cdot\hat{\boldsymbol{\omega}})\cdot\delta(\Phi) = \mathrm{M}_\Omega\cdot\delta(\Phi_\Omega) \geq \hbar \qquad (24)$$

When measuring angular velocity using two components of a ring standing wave in classical optical-physical scheme, a multiplier "1/2" is added to the right side (23), and a multiplier "2" is added to the left side of the inequality (24), correspondingly.

2.2 Additive Error of the "Scale Factor" of LG

We found a systematic error of the LG in the form of an additive decrease in the LG "scale factor" due to the non-planar phase front of a ring standing wave in the resonator.

International Journal of Current Science Research and Review
ISSN: 2581-8341
Volume 07 Issue 07 July 2024
DOI: 10.47191/ijcsrr/V7-i7-54, Impact Factor: 7.943
IJCSRR @ 2024
www.ijcsrr.org

Section 2.1 shows that the gyroscopic effect in a laser gyroscope determined by the presence of the angular momentum of a ring standing wave (wave packet) in a ring laser. Moreover, according to the value (7), the LG scale factor is determined by the doubled angular momentum (8) of the ring radiation wave in units of *h*, averaged along the axial contour of the annular resonator. Previous formulas are derived for wave with a wave vector $\boldsymbol{k} = (2\pi/\lambda)\hat{\boldsymbol{l}}$, where $\hat{\boldsymbol{l}}$ is ort along the axial contour of the resonator.

Let the axis of rotation, perpendicular to the plane of the axial contour of the annular resonator be the *Y* axis; let the direction of radiation propagation be the *Z* axis, and the axis, perpendicular to the *Y* axis, in the plane of the axial contour be the *X* axis. In a real ring laser resonator, the wave front has certain radii of curvature $(R_{x,y})$ at each point of the resonator contour, in the *XOZ* and *YOZ* planes. They are determined by confocal parameters $(b_{s,m})$ and constriction coordinates $(z_{s,m})$ in mutually perpendicular (sagittal and meridional) planes, as in [20]

$$R_{x,y}(z) = z\left[1 + \left(\frac{b_{s,m}}{z - z_{s,m}}\right)^2\right] \qquad (25)$$

Accordingly, in the sagittal and meridional planes, the radii of the constrictions $(\rho_{x,y})$ in each point (z) on the resonator axis are equal

$$\rho_{x,y}(z) = \rho_{0(x,y)}\left[1 + \left(\frac{z - z_{s,m}}{b_{s,m}}\right)^2\right]^{1/2}. \qquad (26)$$

In (25) and (26) confocal parameters $(b_s$ and $b_m)$ are the radii of the diffraction divergence of the beam in each of the planes *XOZ* and *YOZ*, respectively. They define it as

$$b_{s,m} = \frac{\pi\rho_{0(x,y)}{}^2}{\lambda} \qquad (27)$$

The wave vector of the beam $\widetilde{\boldsymbol{k}}$ determines the change in the phase of the wave by the unit of the coordinate change in the direction of wave propagation. Then, when propagating along $\boldsymbol{Z}$:

$$\widetilde{\boldsymbol{k}} = \frac{\partial\Phi}{\partial z}\hat{\boldsymbol{z}}\,, \qquad (28)$$

where Φ is the phase of the beam, and $\hat{\mathbf{z}}$ is ort in the direction of its distribution.

The moment of pulse with such $\widetilde{\boldsymbol{k}}$ is, obviously, equal

$$\tilde{\boldsymbol{\mu}} = \hbar[\mathbf{r} \times \widetilde{\boldsymbol{k}}]. \qquad (29)$$

They can show that for the first axial (main) mode in immovable resonator [20] equal

$$\Phi = \left[kz - \eta(z) + \frac{kx^2}{2R_x(z)} + \frac{ky^2}{2R_y(z)}\right], \qquad (30)$$

where, as usual, $\left(k = \frac{2\pi}{\lambda}\right)$ and

$$\eta(z) = \frac{1}{2}\operatorname{arctg}\left(\frac{z - z_s}{b_s}\right) + \frac{1}{2}\operatorname{arctg}\left(\frac{z - z_m}{b_m}\right) \qquad (31)$$

International Journal of Current Science Research and Review
ISSN: 2581-8341
Volume 07 Issue 07 July 2024
DOI: 10.47191/ijcsrr/V7-i7-54, Impact Factor: 7.943
IJCSRR @ 2024
www.ijcsrr.org

With $\{0 \le x \le \rho_x;\ 0 \le y \le \rho_y;\ 0 \le z \le L_1\}$, where L_1 is the length of the resonator section on which the phase front is not flat. Considering (28) and (30), the wave vector of the beam

$$\widetilde{\boldsymbol{k}} = \left\{k\left[1 - \frac{x^2}{2R_x{}^2(z)} \cdot \frac{dR_x(z)}{dz} - \frac{y^2}{2R_y{}^2(z)} \cdot \frac{dR_y(z)}{dz}\right] - \frac{d}{dz}[\eta(z)]\right\} \cdot \hat{\boldsymbol{z}} \qquad (32)$$

If the curvature of the phase front is of the first order of smallness, when $\{(x^2/2R_x{}^2(z)) << 1;\ (y^2/2R_y{}^2(z)) << 1\}$ and $\left\{\frac{d}{dz}R_x(z);\ \frac{d}{dz}R_y(z)\right\}$ changing slightly on (z), then the wave vector

$$\widetilde{\boldsymbol{k}} = \left\{k - \frac{1}{2} \cdot \frac{d}{dz}\left(\operatorname{arctg}\left(\frac{z-z_s}{b_s}\right) + \operatorname{arctg}\left(\frac{z-z_m}{b_m}\right)\right)\right\} \cdot \hat{\boldsymbol{z}} \qquad (33)$$

Accordingly, the moment of pulse (29) will take the form

$$\widetilde{\boldsymbol{\mu}} = \hbar[\mathbf{r} \times \boldsymbol{k}] - \frac{\hbar}{2}[\mathbf{r} \times \hat{\boldsymbol{z}}] \cdot \frac{d}{dz}\left(\operatorname{arctg}\left(\frac{z-z_s}{b_s}\right) + \operatorname{arctg}\left(\frac{z-z_m}{b_m}\right)\right). \qquad (34)$$

Similarly, to (4-8), we define in (35) for two waves in an annular resonator the frequency difference corresponding to vectors (33) and (34):

$$\Delta\tilde{\nu} = \frac{2\boldsymbol{\Omega}}{\lambda L}\oint[\mathbf{r} \times d\mathbf{l}] - \left(\frac{\boldsymbol{\Omega}}{2\pi L_1} \cdot \int_0^{L_1}\left\{\frac{d}{dl}\left(\operatorname{arctg}\left(\frac{l-z_s}{b_s}\right) + \operatorname{arctg}\left(\frac{l-z_m}{b_m}\right)\right)\right\}[\mathbf{r} \times d\mathbf{l}]\right) \qquad (35)$$

In (35), the integral along the closed axial contour of the resonator for the second term was divided into an integral in the section (0; L_1) of the resonator due to the non-planar phase front, and the rest along the sections of the resonator with a flat front, where the confocal parameters are infinity, and the value (31) is zero.
Considering (5) and (8), we transform (35) in the second integral

$$[\mathbf{r} \times d\mathbf{l}] = 2d\mathbf{S} = 2dS \cdot d\hat{\mathbf{s}} = R_{eff} \cdot dl \cdot d\hat{\mathbf{s}} \qquad (36)$$

As usual, in (36) it is indicated: $d\hat{\mathbf{s}} = [\hat{\mathbf{r}} \times d\hat{\mathbf{l}}]$ and $\left(R_{eff} = \frac{2S}{L} = \frac{2dS}{dl}\right)$. If we write down the decrease in the frequency difference (35) due to the flat phase front on the section of the axial contour L_1 in the form

$$\delta(\Delta\tilde{\nu}) = \delta\widetilde{K}(\hat{\mathbf{s}} \cdot \boldsymbol{\Omega}) \qquad (37)$$

where $\delta\widetilde{K}$ is the change in the LG scale factor due to the flat phase front in the L_1 section. Then, taking into account (36), we obtain the expression

$$\delta\widetilde{K} = -\frac{R_{eff}}{2\pi L_1}\left\{\operatorname{arctg}\left(\frac{L_1-z_s}{b_s}\right) + \operatorname{arctg}\left(\frac{L_1-z_m}{b_m}\right) + \operatorname{arctg}\left(\frac{z_s}{b_s}\right) + \operatorname{arctg}\left(\frac{z_m}{b_m}\right)\right\}. \qquad (38)$$

In (38), integration has already been performed, and L_1 is the length of the section of the resonator contour on which the phase front of the radiation is slightly different from the plane front. On condition $(-1 \le x \le 1)$ it is true the decomposition

International Journal of Current Science Research and Review
ISSN: 2581-8341
Volume 07 Issue 07 July 2024
DOI: 10.47191/ijcsrr/V7-i7-54, Impact Factor: 7.943
IJCSRR @ 2024
www.ijcsrr.org

$$\operatorname{arctg}(x) = x - \frac{x^3}{3} + \frac{x^5}{5} - \frac{x^7}{7} + \cdots \quad . \qquad (39)$$

Substituting (39) into (38), we obtain, in the first approximation, the decompositions for functions $\left\{\operatorname{arctg}\left(\frac{L_1 - z_{s,m}}{b_{s,m}}\right);\ \operatorname{arctg}\left(\frac{z_{s,m}}{b_{s,m}}\right)\right\}$, that the change in the LG scale factor due to the non - flatness of the phase front in the L_1 section of the resonator is equal to

$$\delta\tilde{K} = -\frac{R_{eff}}{2\pi} \cdot \left({b_s}^{-1} + {b_m}^{-1}\right). \qquad (40)$$

The value of L_1 decreases after integration and decomposition. For several sections of a non-planar front with certain confocal parameters, the corresponding values (40) will add up.

As we can see from (40), long-focus mirrors are necessary not only for the Q-factor of the ring laser resonator, but also for the stability of the sensitivity axis and the LG scale factor.

The larger are values of confocal parameters in the resonator, the smaller is additive error of the LG scale factor at any angular velocity of rotation. However, with infinite confocal parameters, when the mirrors are flat, the resonator becomes unstable.

2.3 Precession of Moment and "Capture Zone"

When the system rotates with a moment of force, there should be (and is observed) a phenomenon of precession of the moment of forces acting on an annular standing wave around the acting angular velocity of rotation **Ω**. The change in the angular momentum **M** of each component of an annular standing wave in a rotating system is associated with its change in the inertial reference frame by the corresponding Galilean transformation, as

$$\frac{d}{dt}(\mathbf{M}) = \frac{d'}{dt}(\mathbf{M}) + [\mathbf{\Omega} \times \mathbf{M}] \qquad (41)$$

where the derivative with a stroke corresponds to a change of the angular momentum in a rotating system. With scalar multiplication of the equation (41) by the vector **Ω**, we obtain the condition for the existence of the LG invariant.

The LG invariant will take the form:

$$\left(\hat{\boldsymbol{\omega}} \cdot \frac{d}{dt}(\mathbf{M})\right) = \left(\hat{\boldsymbol{\omega}} \cdot \frac{d'}{dt}(\mathbf{M})\right) = \text{invariant} \qquad (42)$$

The equation (42) allows precession of the vector $d(\mathbf{M})/dt = \dot{\mathbf{M}}$ around the ort $\hat{\boldsymbol{\omega}}$ of the angular velocity vector **Ω** of the LG rotation.

At the same time, author simulated polar conditions on a rotary gyroscopic installation (Fig. 4), when the total vector **Ω** of the rotary installation and the Earth (at the Moscow latitude it is ≈ 8.4 °/ hour) is almost parallel to the vector $\dot{\mathbf{M}}$, and the rotary installation was turned on before the LG was turned on.

International Journal of Current Science Research and Review
ISSN: 2581-8341
Volume 07 Issue 07 July 2024
DOI: 10.47191/ijcsrr/V7-i7-54, Impact Factor: 7.943
IJCSRR @ 2024
www.ijcsrr.org

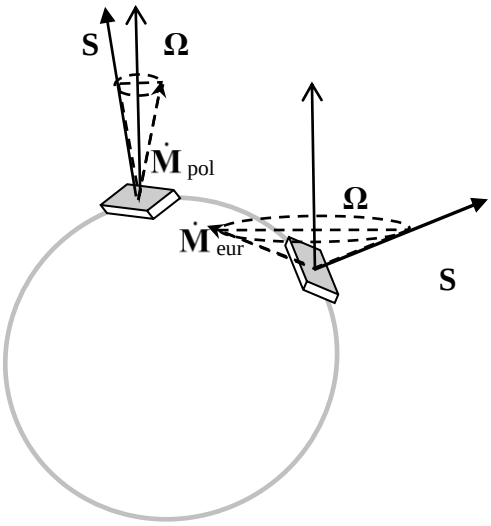

Fig. 4. Precession of the moment vector of forces acting on one of the components of the ring standing wave. Ring resonators are fixing horizontally in the Polar (pol) and European (eur) parts of the globe.

Once LG was turned on, the precession of the vector $\dot{\mathbf{M}}$ was starting around the vertical axis of rotation. Further, when we quickly (much less than a day) reduced the angular velocity of the turntable, the output signal of the LG has decreased linearly, however was not "captured".

With a decrease in the angular velocity of the rotary gyroscopic installation, the precession of the vector $\dot{\mathbf{M}}$ continued around the sum of the angular velocity vectors – of the small rotation of the rotary gyroscopic installation and of the daily rotation of the Earth.

However, the vector $\dot{\mathbf{M}}$ itself moved away from the vertical with a small angular velocity. The "capture zone" proved to be less than the lower limit of the angular speeds of the rotary installation stand.

If the installation stand of LG is attached to the Earth (including as a pendant or on a mercury cushion) acting on the LG before it is turned on, then vector $\dot{\mathbf{M}}$ starts at an extreme position.

In Fig. 4, the precession of the vector $\dot{\mathbf{M}}$ begins around the vector of the daily angular velocity of the Earth's rotation $\boldsymbol{\Omega}$ at an angle $\delta = 90° - \lambda$; where λ is the geographical latitude of the terrain of the horizontal location of the LG, in the direction opposite to rotation.

The "zone angle ζ" between vector $\dot{\mathbf{M}}$ and the axis $\hat{\mathbf{s}}$ characterizes the phenomenon of precession.

With the horizontal placement of the LG on the Earth, the zone angle changes from $\zeta_{min} = 180° - 2\lambda$; to $\zeta_{max} = 0°$ within a day. Accordingly, the "scale factor" of the LG varies from a minimum to a maximum value for a given location. Thus, we propose that with the use of LG it is possible to measure the geographical latitude of an area. And by placing the plane of the LG ray contour vertically on the Earth, in extreme positions along the zone angle ζ, you can find the direction of longitude, or the North-South axis. It is known [17] that some companies carried out the final assembly of manufactured laser gyroscopes in the polar Canada. The empirical assembly was performed there, because the axis of the angular velocity of the Earth's daily rotation in the polar region is almost perpendicular to the plane of the axial contour of the resonator during the assembly and adjustment of laser gyroscopes. Furthermore, it is easier to ensure and precisely control the horizontal placement of the LG.

By the "scale factor" of LG, some mean a constant. Without taking into the account the precession of the vector of moment of force around $\boldsymbol{\Omega}$, the LG output signal is determined by their scalar product.

International Journal of Current Science Research and Review
ISSN: 2581-8341
Volume 07 Issue 07 July 2024
DOI: 10.47191/ijcsrr/V7-i7-54, Impact Factor: 7.943
IJCSRR @ 2024
www.ijcsrr.org

It was found [17] that with the precession LG "scale factor" defined by the projection of **M**(*t*) on **S**. The direction of the area vector **S** has the same meaning as the direction of the area vector **S** in the magnetic moment of an elementary frame with a current.
Most developers still associate the "capture zone" of LG exclusively with the scattering of light on low-quality mirrors, which is incorrect. It follows from our research that it is usually much smaller than the declared one. For example, less than 0.1 Hz instead of 1 kHz.

3. LINEAR RESONATOR BASED DEVICES

Linear resonator based devices with an alteration of the dimensions of light pathlength.

These known devices based on resonator dimension altering and Doppler phenomena. The element of measurement system additionally disposed on the moving object characterizes them. At the same time, other parts of the measurement system are disposed on a motionless environment. This group of devices has common generic subject matter such that altering of dimension of the sensitive pathlength as dynamic response.

Linear resonator based devices with an alteration of the media parameters.

These devices based on the alteration of some parameters of the media in the resonator, as density or birefringence in tensioned fiber, caused by the forced movement due to its specific properties, e.g. inertia. This group of devices has common generic subject matter such that altering of the material parameters of the sensitive pathlength as dynamic response.
All devices of mentioned above groups include necessarily added mechanic or electromagnetic subsystems and non-controlled nonlinear parts on the output characteristics.

3.1 Autonomous Accelerometer Based on Rigid Linear Laser Resonator

In earlier studies of nonlinear optics phenomena and measurements of laser intensity [1, 17], the author observed the phenomena of changes in the space-temporal characteristics of laser beams. For example, as in Fig. 5.
When the laser was moving, the intensity on the opposite mirrors changed in the opposite phase. Fig. 5 shows the change in the spatial characteristics of laser radiation with uneven movement of its phase structure along the black dashed line. The solid line with arrows represents the radiation before the interaction. Dotted red lines with arrows represent the permitted radiation directions in uneven motion.
The intensity and spatial structure of the "single-mode" radiation varied with the uneven movement of the rigid resonator by significant values (from 5%) that exceeds the minimum recorded values and did not correspond to the accuracy class of the used measuring instruments and the relative stability of the electronic subsystems.

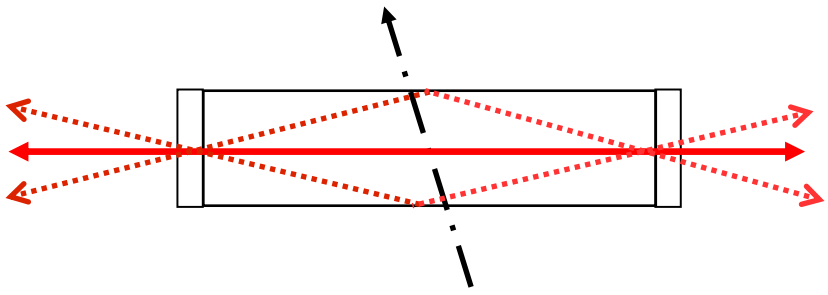

Fig. 5. Optical scheme of changes in the spatio-temporal characteristics of radiation with uneven movement of its resonator along the dashed axis.

In [13-16] we have considered the motion of a field without charges in space under the action of external forces that simultaneously shift the elements of the radiation frame. The parameters of the motion of the framing elements fixed on the object are independently determined through the parameters of the radiation and its source if the field, moving as a whole, has a "phase skeleton" unchanged during the movement.
In our previous works [21-40] accompanying phenomena, prototypes of autonomous resonatory sensors (ARS), theoretical explanation of experimental results and connection with other phenomena, applications, and main advantages of using such sensors

International Journal of Current Science Research and Review
ISSN: 2581-8341
Volume 07 Issue 07 July 2024
DOI: 10.47191/ijcsrr/V7-i7-54, Impact Factor: 7.943
IJCSRR @ 2024
www.ijcsrr.org

have been considered. We used term “autonomous resonatory device” (ARD) in the previous works and then we will use term “autonomous resonatory sensor” (ARS), as in our patent [21].
We sought a joint solution for three equations: energy operator equation (43), action operator equation (56), and wave equation (50) with the corresponding transformations (43.1-2) of coordinates in a moving frame of reference.

$$\hat{\varepsilon} = \hat{\varepsilon}_0 - \left(\boldsymbol{\Omega} \cdot \hat{\mathbf{P}}\right). \qquad (43)$$

We have considered a complex phase as a function of a state. We assumed that the uneven motion of the light source leads to the appearance of a complex phase in the radiation field in its own frame of reference, determined by the acceleration of source and spatial parameters of the phase structure of the source. There was a nonlinear change in the intensity of radiation and the appearance of additional, non-diffraction beams during the movement of the resonator. These assumptions we confirmed experimentally and theoretically.
The main difference between our ARS and Sagnac effect based laser gyro (other than ARS is an accelerometer, and LG is a gyroscope) is the shape of the sensing element: a linear standing light wave in ARS instead of the ring standing light wave in LG. For the components of a standing wave in a linear laser resonator, we used a relation (43) similar to equation (2) in the operator form. From the problem of eigenfunctions–eigenvalues we obtained a complex phase in and around an unevenly moving resonator.

3.2 Radiation Phase Equation for Accelerated Rigid Linear Laser Resonator

The allowed directions and frequencies of radiation in an unevenly moving linear laser resonator are considered. All elements of the resonator shifted when moving together according to the Galilean transformations:

$$\vec{r}_0 = \vec{r} + \vec{S}(t), \qquad (43.1)$$

$$t_0 = t. \qquad (43.2)$$

Here in (43.1) $\vec{r}_0$ - is the radius vector of a point in the reference frame of an inertial observer, $\vec{r}$ - is the radius vector of the same point in a non-inertial reference frame associated with a resonator, and $\vec{S}(t)$ - is the shifting vector of the resonator relative to the inertial observer. Time in (43.2) does not change. In accordance with (43.1-2), the “nabla” operator in the resonator system is equal to

$$\vec{\nabla} = \left(\frac{\partial}{\partial \vec{r}}\right)_t = \left(\frac{\partial}{\partial \vec{r}_0}\right)_{t_0} \cdot \left(\frac{\partial \vec{r}_0}{\partial \vec{r}}\right)_t + \left(\frac{\partial}{\partial t_0}\right)_{\vec{r}_0} \cdot \left(\frac{\partial t_0}{\partial \vec{r}}\right)_t. \qquad (44)$$

Taking into account the vector equation (43.1), the vector derivative in the operator relation (44) is determined by the matrix

$$\left(\frac{\partial \vec{r}_0}{\partial \vec{r}}\right)_t = \begin{pmatrix} \left(\frac{\partial x_0}{\partial x}\right)_{yzt} & \left(\frac{\partial x_0}{\partial y}\right)_{xzt} & \left(\frac{\partial x_0}{\partial z}\right)_{xyt} \\ \left(\frac{\partial y_0}{\partial x}\right)_{yzt} & \left(\frac{\partial y_0}{\partial y}\right)_{xzt} & \left(\frac{\partial y_0}{\partial z}\right)_{xyt} \\ \left(\frac{\partial z_0}{\partial x}\right)_{yzt} & \left(\frac{\partial z_0}{\partial y}\right)_{xzt} & \left(\frac{\partial z_0}{\partial z}\right)_{xyt} \end{pmatrix} = \begin{pmatrix} 1 & 0 & 0 \\ 0 & 1 & 0 \\ 0 & 0 & 1 \end{pmatrix}. \qquad (45)$$

Then in operator (44), the partial derivative of time in the resonator’s own reference frame is

$$\left(\frac{\partial t_0}{\partial \vec{r}}\right)_t = \mathbf{0}. \qquad (46)$$

Operator (44), taking into account (45) and (46), does not change and has the form

$$\vec{\nabla} = \left(\frac{\partial}{\partial \vec{r}}\right) = \left(\frac{\partial}{\partial \vec{r}_0}\right) = \vec{\nabla}_0. \qquad (47)$$

International Journal of Current Science Research and Review
ISSN: 2581-8341
Volume 07 Issue 07 July 2024
DOI: 10.47191/ijcsrr/V7-i7-54, Impact Factor: 7.943
IJCSRR @ 2024
www.ijcsrr.org

Symbol $\vec{\nabla}_0$ in (47) and then – is the "nabla" operator in any inertial frame of reference. On the other hand, the partial derivative in time in a linearly moving proper reference frame is equal

$$\left(\frac{\partial}{\partial t}\right)_{\vec{r}} = \left(\frac{\partial}{\partial \vec{r}_0}\right)_{t_0} \cdot \left(\frac{\partial \vec{r}_0}{\partial t}\right)_{\vec{r}} + \left(\frac{\partial}{\partial t_0}\right)_{\vec{r}_0} \cdot \left(\frac{\partial t_0}{\partial t}\right)_{\vec{r}}. \qquad (48)$$

It is obvious that from (43.1-2) we have in the ratio (48) and: $(\partial t_0/\partial t) = 1$; $(\partial \vec{r}_0/\partial t) = \dot{\vec{S}}(t)$.

The partial derivative in time in a linearly moving proper reference frame will take the form of the operator relation

$$\left(\frac{\partial}{\partial t}\right)_{\vec{r}} = \left(\frac{\partial}{\partial t_0}\right)_{\vec{r}_0} + \left(\dot{\vec{S}}(t) \cdot \vec{\nabla}_0\right). \qquad (49)$$

Then everywhere $(t_0 = t)$. Here in equation (49) $\vec{r}$ - is the radius vector of a point in a non-inertial reference frame that fixed relative to the resonator, $\vec{r}_0$ - is the radius vector of the same point in the reference frame of an inertial observer, and $\vec{S}(t)$ -is the time-dependent only displacement vector of the resonator relative to the inertial observer.

Taking into account the transformations (47) and (49) when moving the non-inertial reference frame, the wave equation will take the form (50):

$$\Delta_0 \Phi = \frac{\varepsilon\mu}{c^2}\left\{\frac{\partial}{\partial t} + \left(\dot{\vec{S}}(t) \cdot \vec{\nabla}_0\right)\right\}^2 \Phi. \qquad (50)$$

The transformed wave equation (50) is not enough to determine the unknown function Φ through three independent (since the movement is arbitrary) variable coordinates S_x; S_y; S_z of the displacement vector.

We assumed that in order to solve the problem of the eigenfunctions–eigenvalues of the operators of the energy and the action of light in a non-inertial frame of reference, it is necessary to supplement equation (50) with the relations (51) and (55), or, respectively, with the equations (54) and (56). With non-relativistic displacement of any physical system having its own momentum $\hat{\vec{P}}$, its energy$(\hat{\varepsilon})$ changes according to

$$\hat{\varepsilon} = \hat{\varepsilon}_0 - \left(\dot{\vec{S}}(t) \cdot \hat{\vec{P}}\right) \qquad (51)$$

The operators in (51) determine the energy $\hat{\varepsilon}$ and $\hat{\varepsilon}_0$ of the electromagnetic field in an unevenly moving resonator and in an inertial observer system, respectively; $\hat{\vec{P}}$ - is pulse operator in the resonator's own reference frame. Equation (51), expressed in energy and pulse operators, has the form:

$$\left[i\hbar \cdot \frac{\partial}{\partial t} + i\hbar\left(\dot{\vec{S}}(t) \cdot \vec{\nabla}_0\right)\right]\Psi = \varepsilon \cdot \Psi. \qquad (52)$$

Eigenfunctions for the problem (52) we are looking as the field vector (53):

$$\vec{E} = \vec{E}_0 \cdot \exp\left[-i \cdot \Phi(t;\vec{r})\right], \qquad (53)$$

International Journal of Current Science Research and Review
ISSN: 2581-8341
Volume 07 Issue 07 July 2024
DOI: 10.47191/ijcsrr/V7-i7-54, Impact Factor: 7.943
IJCSRR @ 2024
www.ijcsrr.org

where $\Phi(t;\vec{r})$ - is the radiation phase for the eigenfunctions of the equations (50) and (52). In units of $\hbar$, equation (52) for energy will take the form.

$$\frac{\partial\Phi}{\partial t}+\left(\dot{\vec{S}}(t)\cdot\vec{\nabla}_0\right)\Phi=\omega(t;\vec{r}). \quad (54)$$

At the same time, when moving any physical system that has its own pulse or momentum, its action also changes. Action $A(t;\vec{r})$ when resonator moving as (43.1) will change as

$$A(t;\vec{r})=A(0;\vec{r})+\left(\vec{S}(t)\cdot\hat{\vec{P}}\right), \quad (55)$$

where the initial action before the uneven movement is equal to $A(0;\vec{r})=A(t=0;\vec{r})$.
For the action in units of $\hbar$ equation (55) will take the form (56) with the initial phase $\Phi(0;\vec{r})$ as

$$\Phi=\Phi(0;\vec{r})-\left(\vec{S}(t)\cdot\vec{\nabla}_0\right)\Phi. \quad (56)$$

Transforming equations (50), (54) and (56) for radiation phase in moving resonator we get the equation

$$\ddot{\Phi}(t;\vec{r})-\left\{\tfrac{1}{2}\dot{S}^2\right\}\Delta_0\Phi(t;\vec{r})=\dot{\omega}-\left(\dot{\vec{S}}\cdot\vec{\nabla}_0\right)\omega-\left(\ddot{\vec{S}}\cdot\vec{\nabla}_0\right)\Phi(0;\vec{r}). \quad (57)$$

In [13-16], solutions of equation (57) are obtained when resonator moves along the direction of the “radiation vector”. Radiation vector introduced in [13; 29-34]). This condition is taken into account in the form

$$t\cdot(\vec{a}\cdot\vec{\nabla})\omega=0. \quad (58)$$

3.3 Optical-Physical Circuits for Accelerated Rigid Linear Laser Resonator

Figure 6 shows the first optical-physical scheme, on which we investigated the compensation of the real and imaginary phases of radiation in a moving resonator. The base plate, with a single-mode laser tube and framing elements fixed on it, was rolled down an inclined plane on fluoroplastic rollers.

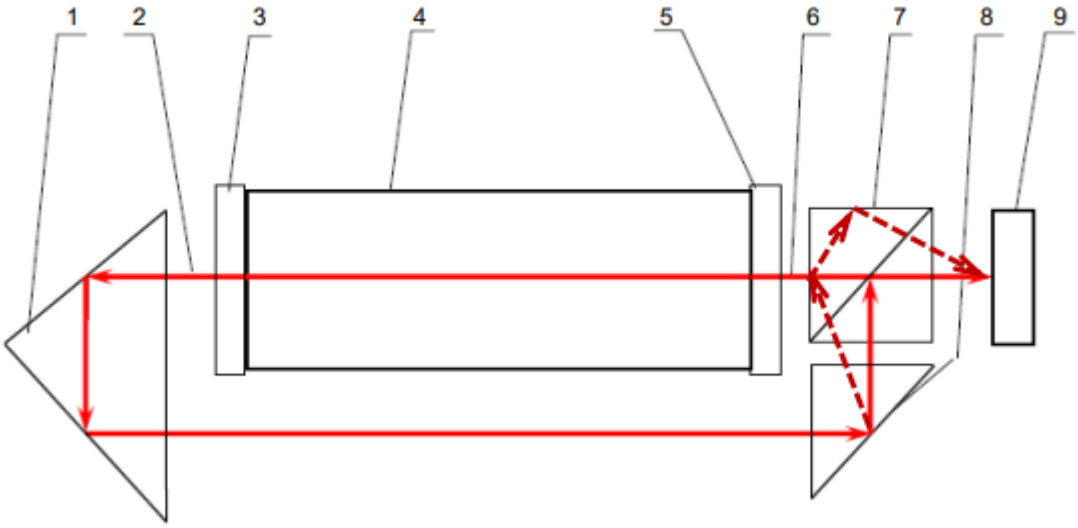

Fig. 6. Optical scheme of a motion-insensitive interferometer based on He-Ne laser (solid arrows). Re-reflections (dotted arrows) on a slightly rotated prism 8 allowed receiving a signal of imaginary parts of phase.

International Journal of Current Science Research and Review
ISSN: 2581-8341
Volume 07 Issue 07 July 2024
DOI: 10.47191/ijcsrr/V7-i7-54, Impact Factor: 7.943
IJCSRR @ 2024
www.ijcsrr.org

Figure 6 shows: 1 and 8 – rotary prisms for the laser beam 2 from the output mirror 3, and the dividing prism 7 compensate its phases with the beam 6 from the output mirror 5 of the same laser 4 to the photodetector 9.

Two cases of combining beam 2 and beam 6 on the photodetector investigated. In both cases, the rays at the exit of mirrors 3 and 5 are in antiphase with phase difference equal to (π), since they propagate in opposite directions.

In the first case, with solid arrows, beam 2 and beam 6, when exiting, respectively, from mirrors 3 and 5, are in antiphase with a phase difference (π). According to the solid arrows, after passing three prisms 1, 8 and 7 with four reflections, the beam 2 hits the photodetector 9 with a shift of the actual phase ($\pi+4\pi = 5\pi$).

In the second case according to Fig. 6 it was obtained by slightly rotated prism 8. After it, beam 2 reflected twice in the dividing prism 7. When the number of reflections for beam 2 changes from four to five due to two "parasitic" re-reflections (dotted arrows), the phase difference in the real parts of the phase becomes equal, for beam 2 and beam 6, to ($\pi +5\pi=6\pi$). This allows observe the signals from imaginary parts of phase that add up in the second case.

Figure 7 shows another optical circuit tested by us, assembled on a single small plate, insensitive to uneven movement. All elements in Fig. 7 are fixed on one plate motionless relative to each other. Here: **P1**, **P2** – rotating prisms, **PhD** – photodetector, **L** – linear laser. Arrows – radiation from the linear laser resonator.

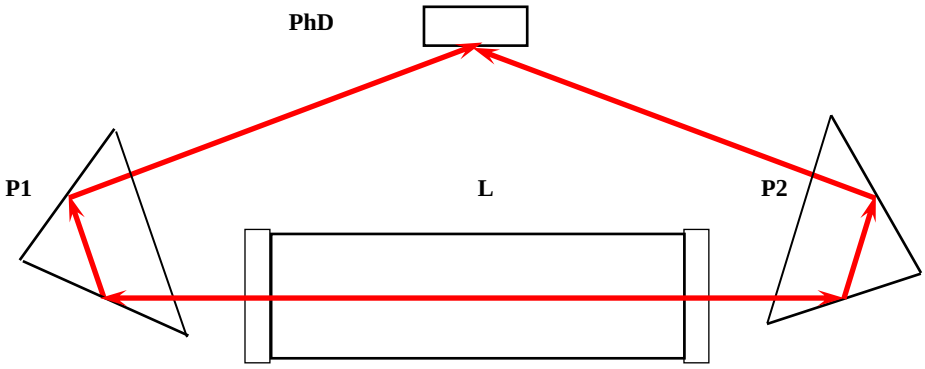

Fig. 7. Insensitive to uneven motion optical scheme for compensation the phases of non-identical beams of a linear laser. (1994, MRTI, RAS).

The device according to the scheme in Fig. 7 remains insensitive to movement when the beams brought together and the photodetector PhD placed at any accessible point of the plate, when the prisms P1 and P2 rotated at different angles on the prototype of Fig. 7 for the measurement period at which the output characteristic can be considered linear.

When one of the output beams of the laser in Fig. 7 is overlapped, the effect under study is observed, but significantly weakened (by 8-10 times) compared to the interference term from two convenient combined beams.

The same ARS with "one-beam interference effect" can be as a single-axis accelerometer or a vibrometer, depending on a method of measurement method and output processing. The ARS also can be used to build a laser gyro without a dead zone, by having a couple of them attached at a fixed, definite distance from each other [26].

Presented devices measure acceleration of actual motion, including constant acceleration compared to piezo effect-based sensors, which are sensing only a change of acceleration of the object. Therefore, presented devices can measure the free fall acceleration of an object it is attached to, contrary to all other types of accelerometers.

Fig. 8 shows the optical scheme of the semiconductor laser based ARS.

In total, the sensor (without a preamplifier, power supplies and control units) contains three parts, including a frameless semiconductor laser, a return mirror and a frameless photodetector. The weight of the sensor together with the housing and the preamplifier is 20 grams.

International Journal of Current Science Research and Review
ISSN: 2581-8341
Volume 07 Issue 07 July 2024
DOI: 10.47191/ijcsrr/V7-i7-54, Impact Factor: 7.943
IJCSRR @ 2024
www.ijcsrr.org

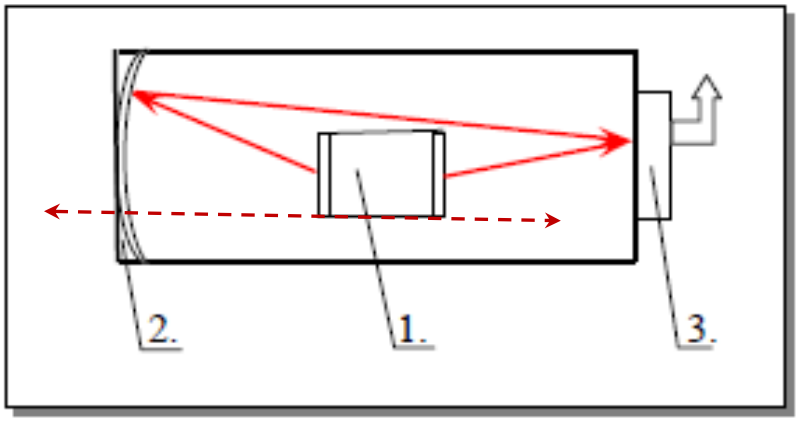

Fig. 8. Optical scheme of ARS based on a semiconductor laser (2000, BAGHRON Co., Ltd)

In Fig. 8 denotes: 1 - uncased semiconductor laser; 2 - return mirror; 3 - photodetector with an output photocurrent. Here solid red arrows present the radiation with uneven motion of the ARS. Dashed arrows present the radiation of a resting ARS. The basic features of the ARSs: «B-1AC» & «B-1AM» listed in the Table 1:

Table 1.

Parameters	***Model B-1AC (ceramic fulfillment)***	***Model B-1AM (metal fulfillment)***	***Analogue in accuracy Model A-4 quartz accelerometer***
Mass	< 0,015 Kg	< 0,020 Kg	0,050 Kg
Dimensions with preamplifier	12 x 12 x 32 mm	Ø12 mm x 32 mm	Ø38 mm x 21 mm
Working range	±12 **g**	±12 **g**	±7 **g**
DC power supply	±5 V; +2 V; 0,1 W	±5 V; +2 V; 0,1 W	±15 V, +9 V; 100 mA
Frequency band of operation	(0÷100) KHz Determined by preamplifier	(0÷100) KHz Determined by preamplifier	(0÷100) Hz
Output signal	Analogue	Analogue	Analogue
Sensitivity	$< 10^{-6}$ ***g*** Determined by photoreceiver	$< 10^{-5}$ ***g*** Determined by photoreceiver	$5 \cdot 10^{-7}$ ***g*** in case of stable ***g***, acts as an accelerometer
Instability of «zero» signal during the movement of object	Does not depend from ***g*** and is determined by electronic units	Does not depend from ***g*** and is determined by electronic units	Not worse than $5 \cdot 10^{-5} \cdot g$ in case of stable ***g*** acting on the accelerometer

CONCLUSIONS

1. The first Michelson and Michelson–Morley experiments allow for a different interpretation.
2. The Sagnac formula is valid only for the resonators with infinite plane phase wavefronts and only when **M**||**Ω**, or when precession is negligible.
3. The angular velocity measurement must be done by measuring the resulting value of the effect of the LG's variable "frequency support" and the measured slowly changing angular velocity at a time when the "scale factor" is almost equal to its maximum calculated value, and the angle ζ between these vectors **M** and **Ω** is small. Thus, for measuring **Ω** in the polar region with horizontally oriented LG, the angle ζ will be small and precession negligible.

International Journal of Current Science Research and Review
ISSN: 2581-8341
Volume 07 Issue 07 July 2024
DOI: 10.47191/ijcsrr/V7-i7-54, Impact Factor: 7.943
IJCSRR @ 2024
www.ijcsrr.org

4. It is possible to measure the geographical latitude of the terrain by placing LG with the axial contour being horizontal to the ground.
5. It is possible to find the direction of geographical longitude, or the North-South axis, by placing LG with the axial contour being vertical to the ground in extreme positions along the zone angle ζ .
6. Additive error of the "scale factor" of LG due to the non-planar wave front of radiation in the resonator has been determined.
7. The maximum sensitivity of LG has been determined.
8. The prototypes of ARS - a new type of linear laser accelerometers that operate without any straining or moving relatively to each other elements have been developed.
9. Depending on the magnitude of the impact and the parameters of the resonator, the response function of the ARS ceases to be noticeable after some time. Thus, ARS's response to a strong constant external impact in the range of $(1\div0.1)\cdot\mathbf{g}$ becomes negligible after about (1÷100) ms, correspondingly. Similarly, a rise time of the first maximum of the ARS response for an acceleration of $\sim10^{-6}\cdot\mathbf{g}$ stays for up to hundreds of seconds at a low amplitude.
10. Proposed ARS can be used in a broad range of applications that require estimation of an object's acceleration, velocity, position, and orientation in space, such as navigation and control systems of moving objects, vehicles, in robotic machinery, tools, and consumer electronics.

ACKNOWLEDGEMENTS

Author would like to thank Prof. V. V. Shevchenko, Co-chair of Moscow Feldman Seminar on Electrodynamics, at Kotelnikov Institute of Radioengineering and Electronics of RAS for valuable discussions and comments, and to pay gratitude and respect to the late Prof. A. A. Rukhadze, former Chair of Theoretical Seminar at Prokhorov General Physics Institute of RAS, and postdoc adviser.

REFERENCES

1. Melkoumian, B. V. "Determination of gas flows of the active medium of a laser gyro" // Uspekhi Prikladnoi Fiziki. - 2016. - V. 4. - №1. - PP. 24-31 (In Russian).
2. Bolotovskiy, B. M., Stolyarov, S. N. // Uspekhi Fizicheskikh Nauk. – 1974. – Vol .114. - Issue 4. - PP. 569-608 (*In Russian*).
3. Born, M., Wolf, E. *Principles of Optics*. - M.: Nauka, 1970 (*In Russian*).
4. Michelson, A. A. // *Amer. J. Sci.* - 1881.- Vol. 22. - P. 20.
5. Michelson, A. A. // *Amer. J. Sci.* - 1887. - Vol. 34. - P. 333.
6. Michelson, A. A., Morley, E. W. // *Amer. J. Sci.* - 1886. - Vol. 31. - P. 377.
7. Sagnac, M. G. //*J.de Phys.Theor. Appl*. – Paris. - 1914. - Vol. 4. - № 1. - PP. 177-195.
8. Sagnac, M. G. // *Comptes Rendus Hebdomadaires des Seances de l'Academie des Sciences.* – Paris. - 1913. - Vol. 157 (25). - PP. 1410-1413.
9. Sagnac, M. G. // *J. Phys. Theor. Appl. – Paris*. - 1913. - Vol. 3. - № 1. - PP. 292-305.
10. Sagnac, M. G. // *J. Phys. Theor. Appl. – Paris*. - 1913. - Vol. **3.** - № 1. – PP. 81-89.
11. Sagnac, M. G. // *Comptes Rendus Hebdomadaires des Seances de l'Academie des Sciences*. – Paris. - 1913. - Vol. 157 (17). - PP. 708-710.
12. Mandelstam, L. I. *Lectures in Optics, Theory of Relativity and Quantum Mechanics.* – M.: Nauka, 1972 (*In Russian*).
13. Melkoumian, B. V. "Radiation vector" of Accelerated Cavity" // Bulletin of the Lebedev Physics Institute. – 2014. - Vol. 41. - No. 2, PP. 35-42.
14. Melkoumian, B. V. "Radiation Phase in the Accelerated Cavity" // Bulletin of the Lebedev Physics Institute. – 2014. - Vol. 41. - No. 7. - PP. 181-184.
15. Melkoumian, B. V. "Conditions for Mode Change of a Rigid Cavity" // Journal of Communications Technology and Electronics. – 2017. - Vol. 62. - No. 8. - PP. 858–864. ISSN 1064-2269 © Pleiades Publishing, Inc. 2017.
16. Melkoumian, B. V. "Radiation Modes of an Accelerated Cavity" // Journal of Communications Technology and Electronics. – 2018. - Vol. 63. - No. 7. - PP. 730–737. ISSN 1064-2269 © Pleiades Publishing, Inc. 2018.
17. Melkoumian, B. V. "LG – gyroscope without rotor with momentum" // Injenernaya Fizika. – 2011. - № 4. – PP. 3-12 (*In Russian*).

International Journal of Current Science Research and Review
ISSN: 2581-8341
Volume 07 Issue 07 July 2024
DOI: 10.47191/ijcsrr/V7-i7-54, Impact Factor: 7.943
IJCSRR @ 2024
www.ijcsrr.org

18. Heer, C. V. // *Phys. Rev.* (1964), Vol. **134**, № 4A, P. A799.
19. Pomerantsev, N. M., Skrotskiy, G. V. // Uspekhi Fizicheskich Nauk – 1970. - Vol. 100. - № 3. - P. 361 (*In Russian*).
20. Kogelnik, H. and Li, T. "Laser Beams and Resonators" // Applied Optics. – 1966. - Vol. 5, No. 10. – PP. 1550-1567.
21. Melkoumian, B. V. "Method and device for autonomous measurement of an irregular movement based on resonatory sensor". Application № 08/568,815; priority date: Dec. 07, 1995; US patent № 5,652,390; date of patent: July 29, 1997. Class: 073-657.000.
22. Melkoumian, B. V. "Gyroscope without rotor with momentum (Review)" // Uspekhi Prikladnoi Fiziki. - Moscow: VIMI, 2016. – Vol. 4. - № 5. – PP. 507-516. (*In Russian*).
23. Melkoumian, B. V. "Scale factor" of laser gyro // Prikladnaya Fizika. – Moscow: VIMI, 2009. - №5. – PP. 137-142 (*In Russian*).
24. Melkoumian, B. V. "Mode change during the movement of the radiation phase skeleton" // Prikladnaya Fizika. – Moscow: VIMI, 2014. - № 3. – PP. 17-21. (*In Russian*).
25. Melkoumian, B. V. "Laser accelerometer based on the autonomous resonatory sensor" // Prikladnaya Fizika. – Moscow: VIMI, 2014. - № 4. – PP. 97-101. (*In Russian*).
26. Melkoumian, B. V. "Application of resonatory sensor of acceleration" // Prikladnaya Fizika. – Moscow: VIMI, 2015. - № 1. – PP. 96-100. (*In Russian*).
27. Melkoumian, B. V. "Accelerated resonator radiation" // Injenernaya Fizika. – 2016. - № 2. – PP. 15-28. (*In Russian*).
28. Melkoumian, B. V. "Radiation intensity of the field with complex phase" // Injenernaya Fizika. – 2016. - № 3. – PP. 81-86. (*In Russian*).
29. Melkoumian, B. V. "Intensity, radiation vector and wave vector of the accelerated resonator mode" // Prikladnaya Fizika. – Moscow: VIMI, 2016. - № 4. – PP. 10-15. (*In Russian*).
30. Melkoumian, B. V. "Imaginary phase of radiation and Doppler frequencies of a moving resonator" // Prikladnaya Fizika. – Moscow: VIMI, 2016. - № 6. – PP. 13-17. (*In Russian*).
31. Melkoumian, B. V. "Conditions of radiation mode dynamic changing" // Bulletin of the Lebedev Physics Institute. – 2016. - Vol. 43. - No. 8. - PP. 244-248.
32. Melkoumian, B. V. "Optodynamics effects" // Proceedings of SPIE. 2000.-Vol. 4348. – SPIE paper № 4348-02.
33. Melkoumian B. V. "Laser accelerometer for guidance and navigation" // Proceedings of SPIE. – 2001. - Vol. 4365. - SPIE paper № 4365-28.
34. Melkoumian, B. V. "Vibrosensor of new generation" // Proceedings of SPIE. – 2002. - Vol. 4627. - SPIE paper № 4627-37.
35. Melkoumian, B. V. "New solutions for autonomous control & navigation" // Proceedings of SPIE. - 2005. - Vol. 5978. – PP. 59781Q-1 - 59781Q-9.
36. Melkoumian, B. V. "Autonomous laser accelerometer for platforms and systems" // SPIE paper № 6736-10. – 2007. – PP. 67360B-1 – 67360B-10.
37. Melkoumian, B. V. "Classical theory of autonomous laser accelerometer" // SPIE paper № 6736-12. – 2007. - PP. 67360D-1 – 67360D-9.
38. Melkoumian, B. V. "Light in non-inertial reference systems with constant phase structure" // The 11th International Workshop on Magneto-Plasma Aerodynamics (Abstracts). – Moscow: Joint Institute of High Temperature of RAS, April 10-12, 2012. – PP. 131-132.
39. Melkoumian, B. V. "Dynamic changing of laser radiation mode" // Proceedings of the 11th Workshop on Magneto-Plasma Aerodynamics. Ed. V. A. Bityurin. – Moscow: Joint Institute of High Temperature of RAS, 2012. – PP. 366-372.
40. Melkoumian, B. V. "New solutions for autonomous control & navigation" // The 12th International Workshop on Magneto-Plasma Aerodynamics (Abstracts). – Moscow: Joint Institute of High Temperature of RAS, March 26-28, 2013. – PP. 126-127.

Cite this Article: Bagrat Melkoumian (2024). Michelson, Morley and Sagnac Experiments Further Elaboration. International Journal of Current Science Research and Review, 7(7), 5175-5193